

## Evaluation of Path Integral Effect on the Local Potential Fluctuation Measurement with HIBP on CHS

LEE Seishu\*, IGUCHI Harukazu, FUJISAWA Akihito, CROWLEY Thomas. P.<sup>1</sup>, HAMADA Yasuji, KOJIMA Mamoru, AKIYAMA Ryuichi, MATSUOKA Keisuke, OKAMURA Shoichi and TAKAHASHI Chihiro

*National Institute for Fusion Science, Toki 509-5292, Japan*

<sup>1</sup>*Rensselaer Polytechnic Institute, Troy, NY 12180-3590, USA*

(Received: 30 September 1997/Accepted: 22 October 1997)

### Abstract

Local and direct probing of plasma interior is considered to be a major advantage of heavy ion beam probe (HIBP) diagnostic. However, in the presence of MHD fluctuations, beam acceleration (or deceleration) may occur due to the magnetic field fluctuation and may change the beam energy. It is called path integral effect. In order to calculate the path integral term, a model vector potential for a cylindrical plasma column is assumed through experimental approaches. In the above analysis, the contribution from path effect is estimated to be less than several percent to the observed space potential fluctuation.

### Keywords:

CHS, HIBP, potential fluctuation, MHD instability, magnetic probe, path integral effect, vector potential

### 1. Introduction

A heavy ion beam probe (HIBP) is a unique diagnostic instrument which can measure local plasma potential and its fluctuations. However, in HIBP for helical devices, the beam travels a certain distance in the toroidal direction and the path integral term should not necessarily be neglected[1]. In order to calculate the path integral term, it is necessary to know the detailed spatial structure of the vector potential, both on the inside and the outside of the plasma. It is not easy to measure it directly by HIBP in the real helical magnetic configuration because of its non-axis-symmetry of the torus. In this paper, the path integral effect is estimated for the HIBP diagnostic during  $m/n=2/1$  MHD oscillation observed in CHS[2], where a model vector potential for a cylindrical plasma column is assumed through experimental approaches. We will estimate the vector potential outside the plasma from the

magnetic probe data. Since we do not have information on the vector potential inside the plasma, we assume the reasonable amplitude in  $q=2$  rational surface which can be connected to the curve for outside the plasma. We consider that this estimation will give us the upper limit of the contribution of path integral term.

### 2. Experiment

The plasma is initially produced by the second harmonic electron cyclotron heating (ECH, 53.2 GHz) and then neutral beam (NB) is injected (co-injection). The port through power is 0.85 MW. The line averaged electron density  $n_e$  is kept low at around  $1.7 \times 10^{19} \text{ m}^{-3}$  by gas puff control and the diamagnetic beta value is constant at 0.2 % during the discharge. The position of the magnetic axis and the magnetic field strength are 0.92 m and 0.9 T, respectively. The rotational

\*Corresponding author's e-mail: leekun@rddfuj.nifs.ac.jp

transform is 0.3 at the center and 1.0 at the periphery. This is a typical configuration where the burst-like MHD mode is observed[3]. Singly charged cesium ions (71.2 keV) are injected into a plasma as a probing beam.

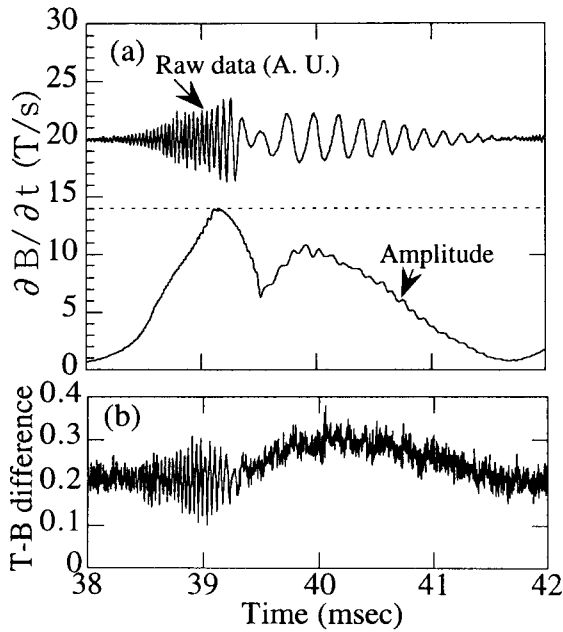


Fig. 1 (a): Time derivative of magnetic fluctuations with a Mirnov coil (upper trace), and its amplitude (lower trace). (b): Typical time variation of the normalized T-B difference during the burst-type MHD instability ( $\rho=0.5$ ).

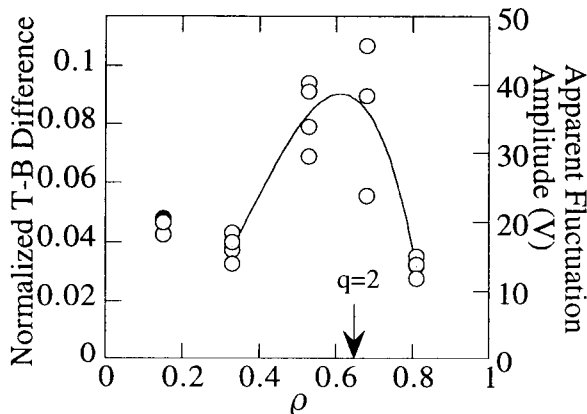


Fig. 2 Normalized T-B difference for each sample positions. Vertical scale on the right hand side is the apparent potential fluctuation amplitude.

Figure 1(a) shows the time variation of magnetic oscillation frequency during a burst cycle. The frequency decreases from about 20 kHz to 5 kHz during a burst cycle. Figure 1(b) shows the normalized top-bottom (T-B) difference of the split plate detector during one MHD burst cycle which is a measure of the space potential. The normalized minor radius  $\rho$  ( $=r/a$ ) of sample position is about 0.5 in these figures. The normalized T-B differences for different radial positions are shown in Fig. 2. Since the burst-type mode changes its amplitude during one burst period, we compare it at its maximum. Although the data points are taken shot by shot, the amplitude can be compared each other, because the fluctuation is very reproducible. The fluctuation level is high at around  $\rho=0.5 \sim 0.7$  where the  $q=2$  rational surface is located.

### 3. Analysis

The probing beam, passing through the plasma gains energy due to acceleration by the electric field along the beam trajectory. It is expressed as follows:

$$\delta W = \int_a^b q(-\nabla\phi - \frac{\partial A}{\partial t}) \cdot dL, \quad (1)$$

where  $\phi$  is the scalar potential,  $A$  is the vector potential,  $a$  and  $b$  are initial and final positions of the beam. When the magnetic oscillations are small, the pass integral term is negligible, and HIBP can measure the local plasma potential. In the presence of strong magnetic oscillations, however, it is necessary to examine this term.

We will estimate the vector potential outside the plasma from the magnetic probe data. For convenience, the toroidal component is only discussed. In a cylindrical coordinate, toroidal component of the vector potential  $A_\zeta$  (outside the plasma) satisfies the Laplace's equation

$$\nabla^2 A_\zeta = \frac{\partial^2 A_\zeta}{\partial r^2} + \frac{1}{r} \frac{\partial A_\zeta}{\partial r} + \frac{1}{r^2} \frac{\partial^2 A_\zeta}{\partial \theta^2} + \frac{\partial^2 A_\zeta}{\partial \zeta^2} = 0 \quad (2)$$

Where  $\zeta$  and  $\theta$  are toroidal and poloidal angle variables, respectively. If the perturbation of  $A_\zeta$  is expanded as

$$A_\zeta = \sum_{m=-\infty}^{\infty} A_{\zeta m, n}(r) \cos(m\theta - n\zeta),$$

Eq.(2) is expressed as the following differential equation for the mode number  $m$ :

$$\frac{\partial^2 A_{\zeta, m}}{\partial r^2} + \frac{1}{r} \frac{\partial A_{\zeta, m}}{\partial r} - \frac{m^2}{r^2} A_{\zeta, m} = 0, \quad (3)$$

where we neglect the  $\zeta$  dependence of the instability. Then it is reasonable to relate  $A_{\zeta, m}$  at the plasma edge

a with  $A_{\zeta,m}$  at the magnetic coil position  $r_c$  as

$$A_{\zeta,m}(a) = \left(\frac{r_c}{a}\right)^m A_{\zeta,m}(r_c). \quad (4)$$

In the cylindrical coordinate, the magnetic fluctuation  $\tilde{B}_\theta$  is represented as

$$\tilde{B}_{\theta,m}(r_c) = -\frac{\partial \tilde{A}_{\zeta,m}(r_c)}{\partial r} \quad (5)$$

The time derivative of perturbed vector potential at the plasma edge can be derived as

$$\frac{\partial \tilde{A}_{\zeta,m}(a)}{\partial t} = \frac{r_c}{m} \left(\frac{r_c}{a}\right)^m \frac{\partial \tilde{B}_{\theta,m}(r_c)}{\partial t} \quad (6)$$

The amplitude of  $\partial B\theta/\partial t$  at  $r_c$  is obtained from the magnetic probe data (Fig. 1). Figure 3 shows the model vector potential profile used here. In order to estimate the maximum value of vector potential term, we have extended the Eq.(6) into plasma interior up to  $q=2$  surface ( $\rho=0.65$ ). Inside of this surface, a constant gradient  $A_\zeta$  is assumed based on  $m=2$  structure.

Then the path integral term can be calculated as follows:

$$\begin{aligned} \delta W &= \sum_{i=1,2} q_i \int \frac{\partial \tilde{A}_\zeta(l)}{\partial t} \cdot dl_{\zeta,i} \\ &= \sum_{i=1,2} q_i \int \frac{\partial \tilde{A}_\zeta(r)}{\partial t} \\ &\quad [-\cos[(m\theta - n\zeta) + m\delta]] \cdot dl_{\zeta,i}(r, \theta), \quad (7) \end{aligned}$$

where  $dl_\zeta$  is the  $\zeta$  component of the primary and secondary beam path length which have been calculated by beam trajectories and is a function of  $r$  and  $\theta$ . In Eq.(7),  $\theta$  dependence is taken as  $\{-\cos(m\theta - n\zeta + m\delta)\}$  just for convenience of calculation, where  $\delta$  represents the phase relation between the beam line and the poloidal mode structure of the instability. The  $n\zeta$  term represents the poloidal mode variation within the HIBP observation area ( $\delta\zeta \sim 22.5^\circ$ ). Figure 4 shows the calculated energy gain as a function of beam location for the sample position of  $\rho=0.5$  and  $\delta=0$ . The total energy changes due to the path integral effect is less than 1.2 V. Summary of the calculation for each sample position is shown in Fig. 5, which shows the ratio of vector potential term to scalar potential term as a function of  $\delta$ . The ratio varies with the phase  $\delta$ , but within several percent. However, it should be noted that the effects from the radial or azimuthal components of the vector potential are not discussed.

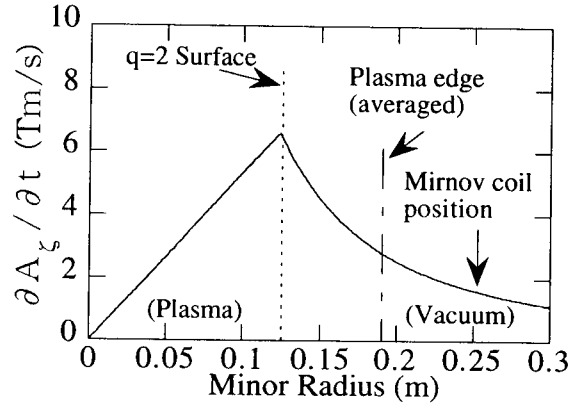


Fig. 3 Model vector potential profile. The curve for plasma outside is estimated from the magnetic probe data.

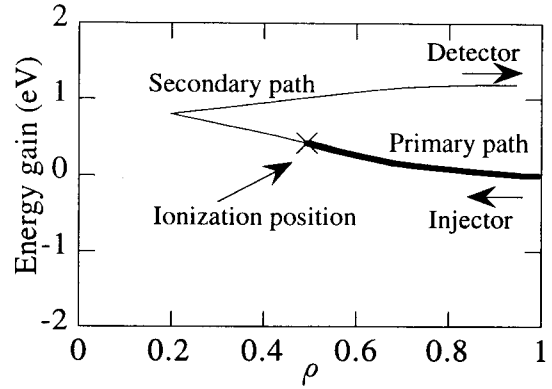


Fig. 4 Energy gain due to the path integral effect along the beam trajectory.

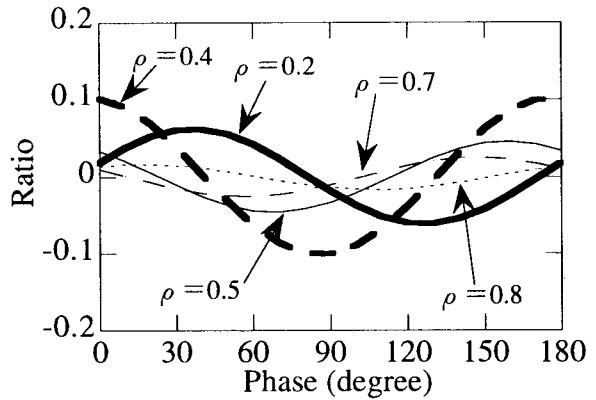


Fig. 5 The ratio of maximum values of vector potential and scalar potential terms for several sample positions. The horizontal coordinate presents the phase relation between the beam trajectory and the poloidal mode structure.

#### 4. Summary

It is shown that the path integral effect on the potential fluctuation measurement is less than several percent for the observed burst type MHD oscillation. The results of above analysis guarantee that Fig. 2 shows the practical profile of scalar potential fluctuation. Then it concludes that the potential fluctuation is large at around  $\rho=0.5\sim 0.7$ , where the  $q=2$  rational surface is located. It is the first time to investigate the path integral effect on potential fluctuation measurement. Although, more accurate analysis is necessary in future work.

#### References

- [1] A. Fujisawa, H. Iguchi, M. Sasao, Y. Hamada and J. Fujita, *Rev. Sci. Instrum.* **63**, 3694 (1992).
- [2] A. Fujisawa *et al.*, *Proc. IAEA Conf. Plasma Physics and Controlled Nuclear Fusion*, 1996, IAEA-CN-64/C1-5.
- [3] S. Sakakibara, H. Yamada *et al.*, *J. Phys. Soc. Jpn.* **63**, 4406 (1994).